

Two dimensional infrared correlation spectroscopy studies of wood-plastic composites with a copolyamide as matrix

M-C. POPESCU*, M. ZANOAGA, Y. MAMUNYA^a, V. MYSHAK^a, C. VASILE

Romanian Academy, "Petru Poni" Institute of Macromolecular Chemistry, 41 A Grigore Ghica Vodă Alley, Iași, Romania

^aInstitute of Macromolecular Chemistry, 48 Kharkivske Shausse, 02160 Kiev, Ukraine

The natural polymer/synthetic polymer combination offers an attractive solution to create environmentally friendly degradable materials, which should not have negative effects on the environment. A modern solution to create such of materials consists in using natural fibres as reinforcement agent in composites applicable in various fields as automotive industry, building, etc. Their performance strongly depends on solid reinforcement-polymer matrix adhesion that determines stress transfer between the phases. Fourier-transform infrared (FT-IR) spectra and generalised two-dimensional (2D) correlation spectroscopy have been applied to analyse the composition-dependent spectral variations in wood thermoplastic composites, emphasising on components' interactions. In the present work the wood-plastic composites with a copolyamide as matrix and different contents, varying from 30% to 70% of wood chips have been studied. Significant modifications are evidenced in 2800-3600 cm^{-1} and 800-1800 cm^{-1} regions. Detailed analysis of the spectra in respect with those of the components and calculated ones indicated that the interaction between wood and copolyamide is relatively strong. The 2D synchronous correlation analysis allows the separation of the bands of wood from those of copolyamide and clearly evidenced new spectral features in composite materials. Moreover, the 2D asynchronous correlation analysis produces cross-peaks those are indicative of the specific interaction or the conformational changes in the blends.

(Received November 2, 2006; accepted February 28, 2007)

Keywords: FTIR and 2D-correlation spectroscopy, Copolyamide, Wood chips

1. Introduction

Generalised two-dimensional (2D) correlation spectroscopy, [1] which is an extension of the original 2D correlation spectroscopy proposed by Noda in 1986 [2-4] has received great attention in the last decades. This novel 2D-correlation method can be applied to analyse the spectral signals that change as functions of not only time but also any other kinds of reasonable physical variables, such as temperature, pressure, concentration, and composition. Generalised 2D correlation spectra emphasise spectral features not readily observable in conventional one-dimensional spectra. It can also probe the specific order of certain spectral events taking place with the development of a controlling physical variable. The type of spectral signals analysed by the newly proposed 2D-correlation method becomes virtually limitless, ranging from IR and Raman spectroscopy to X-ray and fluorescence spectroscopy. Many applications of generalised 2D correlation spectroscopy have been reported, including temperature-dependent spectral variations, [5-10] concentration-dependent spectral changes [11,12] and 2D IR and Raman heterospectral correlation analysis, [13] as well as 2D near-infrared (NIR) and mid-infrared heterospectral correlation analysis [14].

Following the pioneering work of Noda [1-4], many research groups have adopted 2D correlation analysis to study e.g. self-associated molecules [15], polymers [16-18], liquid crystals [19-21], Langmuir-Brogett films [22] and biological molecules, such as peptides [9] proteins [23-25], cellulose and wood [26-31], etc.

The birth of the wood polymer composite (WPC) industry involved the interfacing of two industries that have historically known little about each other and have very different knowledge, expertise, and perspectives. The industry was reluctant to use wood fillers, because these fillers are inexpensive, renewable, biodegradable, have lower density than mineral fibres, and are less abrasive to processing equipment than conventional fillers. Most plastic processors ignored wood fillers because of their low bulk density, low thermal stability, and tendency to absorb moisture.

Today, there is a considerable commercial interest in thermoplastic composites filled with wood waste, due to potential opportunities of combining the attractive characteristics and properties of both components. The product developed has the aesthetic appearance of wood and the processing capability of thermoplastics. The material can be considered as an easily attainable (natural) option, is competitive as far as price is concerned and convenient for a wide range of applications. Raw material costs outstanding product properties and new design possibilities are the drivers of these new composites.

In many cases either the fibres (such as wood, flax, hemp, jute, kenaf) or the polymers (such as polyethylene, polypropylene, polyamide, polyvinyl chloride, polystyrene), can come from residues and vegetable materials, respectively.

The total market for WPCs in North America is forecast to grow at an average annual rate of 14% through the remainder of the decade. In Western Europe the market for WPCs is still in its infancy. The current European WPC producers come from a variety of backgrounds, with

28% being completely new companies, 22% having their core business in PVC profiles, 22% being timber companies and 11% being recycling companies. The European WPC market has so far developed most strongly in Germany, with the supply structure numerically strongest in Germany and the UK. Overall, the Western European market for WPCs is forecast to grow at 18% per year through 2010. The diversity of industry rivals in both North America and Western Europe will continue to help the market grow [32].

Among from drawbacks of the composites with natural fillers, the limited thermal stability, and poor adhesion between the fillers and polymer matrix and irregular filler distribution are most important. The performance of polymeric matrix composites reinforced with wood waste strongly depends on solid wood-polymer matrix adhesion to allow stress transfer between the phases. Poor interfacial adhesion results from a different chemical nature of the components: cellulose fibres from wood are hydrophilic, whereas thermoplastic matrices are predominantly hydrophobic.

New formulations and processing methods as well as a better understanding of material behaviour and composite performance will lead to more efficient WPCs and new applications. A detailed understanding of interfacial interactions of WPCs is needed to optimise the processing technologies, and thus increase the usefulness of wooden material as a constituent of composites.

This work deals with the study of the specific interactions at interface between WPCs by FT-IR and 2D IR correlation spectroscopy.

2. Experimental

2.1 Materials

Copolyamide (coPA) used as matrix for the composites was obtained by direct melt polycondensation, through a "one-pot" technology described elsewhere [33, 34]. The main characteristics of polymer matrix are: chemical composition – a ternary statistic copolymer of adipic acid and sebacic acid with hexamethylene diamine and ϵ -caprolactame 6/6.6/6.10; molecular weight, $M_n = 2800-3000$ g/mol; polydispersity index, $I (M_w / M_n) = 1.050$; granulation: 0.3-0.5 mm; density (at 23 °C): 1.11 g/cm³; crystallinity: 58 %; melt flow index (MFI, 2.16 daN/190°C) = 18-20 g/10 min; melting temperature interval: 125-135 °C.

Wood chips. As wood component, pine chips were used as waste from a furniture manufacturing. The average chip dimensions varied from 0.2 to 2 mm. Prior mixing the wood waste was dried at 60 °C for one hour, and sieved retaining the fraction with dimensions less than (0.5 mm).

2.2 Obtaining of composites

As it has been already mentioned, manufacture of composites was realised in a two-step process, due to the difference of density between the two materials [35-37].

Three different weight fractions of wood chips were used for the preparation of composite materials from 30 up to 70% of the total weight of the composite. On the first stage, dry wood chips and polymer were mixed in a determined ratio, then the mixture was homogenised in an extruder with the temperature of 160°C. The polymer-wood mixture was transformed by extrusion into pellets with a size of 2-3 mm. On the second stage, the pellets were pressed in a metallic compression mould (temperature = 150°C, for 3 min., at a pressure of 20 kg/cm²) into sheet. After pressing, the mould was placed in the cold press where was cooled to room temperature, under the same pressure.

The samples used in IR spectroscopy were obtained by mechanical grinding into powder having 200 μ m diameters, and then were mill-mixed with KBr in order to obtain a good homogenization.

2.3. Investigation methods

2.3.1 FT-IR Spectroscopy

FT-IR spectra were recorded at room temperature on solid samples in KBr pellets by means of a DIGILAB, Scimitar Series, USA spectrometer with a resolution of 4 cm⁻¹. The concentration of the sample in the tablets was constant at 5 mg/500 mg KBr. Processing of the spectra was done by means of Grams/32 program (Galactic Industry Corp.).

3.3.2 2D correlation spectroscopy

2D FT-IR correlation intensities were calculated using an own MATLAB program using the generalized 2D-correlation method developed by Noda [2]. In order to investigate composition dependent spectral changes of WPCs under study the FT-IR spectra of wood and its composites with coPA were divided into two sets: set A and set B [38]. Set A is formed by the FT-IR spectra of *wood, 60% wood - 40% coPA*, and *40% wood-60% coPA*. Set B is constitutes of FT-IR spectra of *40% wood-60% coPA, 30% wood-70% coPA* and *coPA*. The spectra in set A and set B was arranged in such order as the intensities of the bands of wood are decreasing while those of coPA are increasing.

In 2D-correlation analysis, two kinds of correlation maps synchronous and asynchronous are generated from a set of dynamic spectra obtained from the modulation experiment [1]. According to [38], using Φ to designate synchronous 2D correlation intensities between two bands, can be written the following relations:

$$\begin{aligned} \Phi [\nu(\text{wood}), \nu(\text{wood})] > 0 \quad \Phi [\nu(\text{coPA}), \nu(\text{coPA})] > 0 \\ \Phi [\nu(\text{wood}), \nu(\text{coPA})] < 0 \quad \Phi [\nu(\text{coPA}), \nu(\text{wood})] < 0 \end{aligned}$$

Based on these relations, is possible to ascribe bands in the spectra of the composites either to wood or to coPA.

An asynchronous correlation peak appears only if the intensity change of two bands at ν_1 and ν_2 has basically dissimilar trends. According to Noda [1] $\Phi[\nu_1, \nu_2] < 0$ and $\Psi[\nu_1, \nu_2] > 0$ imply that the intensity change at ν_1

occurs at higher wood content compared to that at v_2 . So do $\Phi[v_1, v_2] > 0$ and $\Psi[v_1, v_2] < 0$. $\Phi[v_1, v_2] < 0$ and $\Psi[v_1, v_2] < 0$ imply that the intensity change at v_1 takes place at lower wood content than that at v_2 . When an asynchronous peak $\Psi[v_1, v_2]$ appears between two bands at v_1 and v_2 , it can be either due to the conformational change of the component polymers in their blends or to the specific interactions between the component polymer [1]. If the sequential order between v_1 and v_2 in set A is reversed in set B, then the band at v_1 and v_2 can be regarded as indicative of the specific interaction between wood and coPA

3. Results and discussion

The spectra of the WPC obtained at room temperature contain all bands corresponding to the two components (Fig. 1). A detail examination of the spectra evidences changes in the 2700–3700 cm^{-1} (Fig. 1a) and 900–1800 cm^{-1} (Fig. 1b) regions.

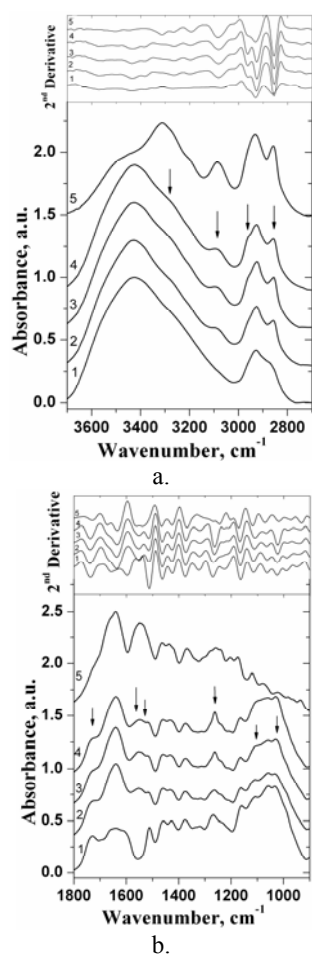


Fig. 1. FT-IR spectra and 2nd derivative of the pure components and blends recorded in 2700–3700 cm^{-1} (a) and 900–1800 cm^{-1} (b) regions: (1) wood, (2) 60 wood/40 coPA, (3) 40 wood/60 coPA, (4) 30 wood/70 coPA and (5) coPA

Spectral modifications occurred in WPC and bands position was evidenced much clearly by the second derivative method. Generally, the secondary derivative IR spectra can obviously enhance the apparent resolution and amplify tiny differences of IR spectrum. The second derivative of the IR spectra (figure 1 a, b) was obtained with the Savitsky-Golay method (second-order polynomial with fifteen data points) using Grams 32 program.

IR spectrum of wood (curve 1) present bands at: 3422 cm^{-1} (corresponding to stretching vibration of OH groups), 2927 and 2875 cm^{-1} (stretching vibration of aliphatic groups), 1736 and 1657 cm^{-1} (corresponding to stretching vibration of C=O groups), 1511 cm^{-1} (C=C stretching of aromatic skeletal), 1268 cm^{-1} (guaiacyl ring breathing, C=O stretch in lignin, C-O linkage in guaiacyl aromatic methoxyl groups), 1160, 1107 and 1057 cm^{-1} (corresponding to C-O symmetric and asymmetric stretching); while IR spectrum of pure CoPA (curve 5) shows the presence of the following peaks: 3449 and 3311 cm^{-1} (corresponding to stretching vibration of OH groups), 3200 and 3085 cm^{-1} (corresponding to stretching vibration of NH groups), 2930 and 2857 cm^{-1} (stretching vibration of C–H groups), 1729 cm^{-1} (stretching vibration of C=O groups), 1640 cm^{-1} (amide I), 1549 cm^{-1} (amide II), 1258 cm^{-1} (amide III) and 935 cm^{-1} (amide IV).

From Fig. 1a can be observed that upon increasing coPA content in the WPC, an increase of the absorbance of the bands at 3311 and 3200 cm^{-1} corresponding to the stretching vibrations (ν) of H-bonded OH groups and NH groups. In addition, an increase of the absorbance of the bands at 2928 cm^{-1} and 2857 cm^{-1} corresponding to the stretching vibrations (ν) of aliphatic groups was evidenced.

In 900–1800 cm^{-1} region the band at 1727 cm^{-1} corresponding to the stretching vibration of C=O group is present in all WPCs. The intensity of this band remains constant independently on the content of wood in the WPC. The band at 1549 cm^{-1} increase and the bands at 1511, 1107 and 1032 cm^{-1} decrease with increasing coPA content in WPC.

With the aim of establishing whether the blending determined spectral changes, the pure components spectra were taken into account and on the basis of additivity law the calculated spectra of the blends were obtained and compared with the experimental ones recorded at room temperature (Fig. 2). For an immiscible blend the additive spectrum is overlapped with the experimental one, while for a miscible or partially miscible blend, differences such as frequency shifts, band broadening, and changes in the intensity of some bands caused by intermolecular interactions between components could appear. The differences could be attributed to some conformational changes too. [39]

For all the studied WPC, one can remark differences between experimental and calculated spectra in the 2700–3700 (Fig. 2a) and 900–1800 cm^{-1} (Fig. 2b) regions.

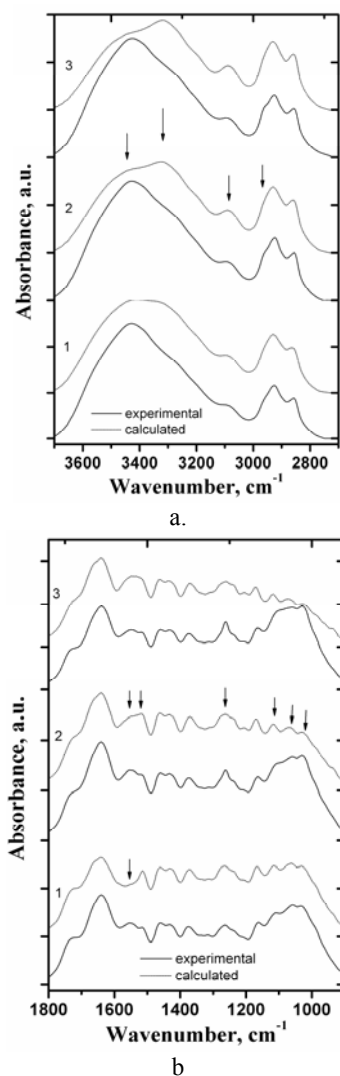


Fig. 2. Experimental and calculated FT-IR spectra in 2700–3700 cm^{-1} (a) and 900–1800 cm^{-1} (b) regions: (1) 60 wood/40 coPA, (2) 40 wood/60 coPA and (3) 30 wood/70 coPA.

For all the studied compositions in 2700–3700 cm^{-1} region the calculated spectra present two bands at 3418 and 3320 cm^{-1} more distinct and at low intensity than in experimental ones (Fig. 2a). The intensity of the band at 3418 cm^{-1} decreases while the bands at 3319 and 3095 cm^{-1} increase with increasing coPA content. In 900–1800 cm^{-1} region, in case of WPC with high content of wood, the band at 1551 cm^{-1} does not appear in calculated spectrum and the band at 1515 cm^{-1} is more intense in calculated spectrum than experimental one.

In the calculated IR spectra of the composites with wood content lower than 50 wt%, the 1551 cm^{-1} band increases with coPA content. At the highest coPA content this band overlaps the 1515 cm^{-1} band, they form a single wide band at 1539 cm^{-1} . In experimental spectra these bands are totally separate and have the same intensity for the 30–60 wt% wood content. The bands at 1114, 1068 and

1029 cm^{-1} in calculated spectra are clearly separated and their intensity is lower than experimental ones while the band at 1264 cm^{-1} is much pronounced in experimental spectra than that from experimental spectra.

The spectral modifications could be explained by partial destruction of intermolecular hydrogen bonds in CoPA and formation of new hydrogen bonds at the interfacial boundary polymer-wood. At the same time, a new type of bonds between polar groups from CoPA (C=O, –NH–) and functional groups of wood (–OH, C–O–) is formed. To elucidate this aspect, further information was obtained from 2D IR correlation spectroscopy.

Bands in the spectral region from 3700–2700 cm^{-1} of wood and coPA are due to aliphatic CH stretching vibrations. In Figs. 3 and 4 are presented synchronous and asynchronous correlation maps of the set A and B for experimental data in this region.

The set A contain wood and two WPCs of 60% wood - 40% coPA, and 40% wood-60% coPA. The synchronous spectrum in 3700–2700 cm^{-1} region of this set is presented in fig 3a. In this spectrum was evidenced seven auto-peaks at 3608, 3350, 3333, 3225, 3158, 3075, 2958, 2916 and 2850 cm^{-1} , nine positive cross-peaks (un-shaded) at 3608 vs. 3333 cm^{-1} , 3608 vs. 3225 cm^{-1} , 3608 vs. 3158 cm^{-1} , 3333 vs. 3158 cm^{-1} , 3075 vs. 2958 cm^{-1} , 3075 vs. 2916 cm^{-1} , 3075 vs. 2850 cm^{-1} , 2958 vs. 2916 cm^{-1} , 2958 vs. 2850 cm^{-1} and 2916 vs. 2850 cm^{-1} and nine negative cross-peaks (shaded) at 3608 vs. 3075 cm^{-1} , 3608 vs. 2958 cm^{-1} , 3608 vs. 2916 cm^{-1} , 3608 vs. 2850 cm^{-1} , 3350 vs. 2850 cm^{-1} , 3158 vs. 3075 cm^{-1} , 3158 vs. 2958 cm^{-1} , 3158 vs. 2916 cm^{-1} and 3158 vs. 2850 cm^{-1} . The assignment of these bands is consistent with the sign of the cross-peaks. The cross-peak is positive for bands due to the same components of blend and negative for bands due to other components.

The bands at 3075 cm^{-1} arise from the coPA. This band has positive correlation with the bands at 2958, 2916 and 2850 cm^{-1} and negative correlation with the bands at 3608, 3225 and 3158 cm^{-1} . This fact indicate that the bands at 2958, 2916 and 2850 cm^{-1} is also due to the coPA whilst bands at 3608, 3225 and 3158 cm^{-1} are due to wood, and that the intensity change of the bands at 3075, 2958, 2916 and 2850 cm^{-1} has the same direction and opposite direction with bands at 3608, 3225 and 3158 cm^{-1} . In similar mode the band at 3350 and 3333 cm^{-1} can be assigned to the wood.

The synchronous spectrum of set B (Fig. 4a) present only one auto-peak at 3433 cm^{-1} , one positive cross-peak at 3433 vs. 3225 cm^{-1} and four negative cross peaks at 3433 vs. 3075 cm^{-1} , 3433 vs. 2950 cm^{-1} , 3433 vs. 2908 cm^{-1} and 3433 vs. 2858 cm^{-1} . Like in previous case the bands at 3075 cm^{-1} has positive correlation with the bands at 2950, 2908 and 2858 cm^{-1} and negative correlation with the bands at 3433 and 3225 cm^{-1} . In consequence the bands at 2950, 2908 and 2858 cm^{-1} is due to the coPA whilst bands at 3433 and 3225 is due to wood.

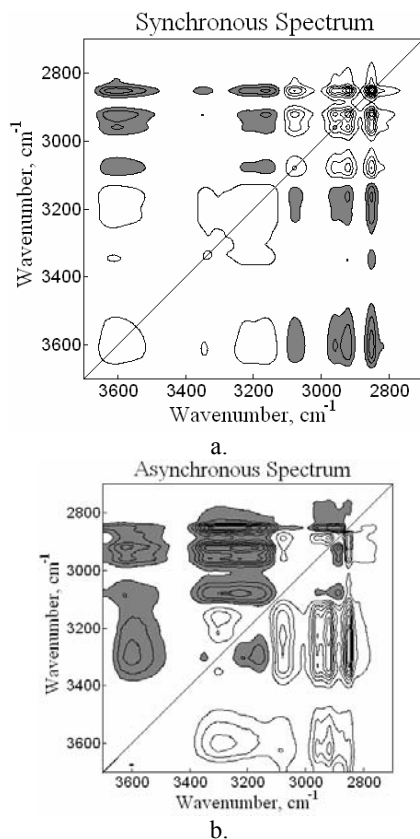


Fig. 3. Synchronous (a) and asynchronous (b) 2D FT-IR correlation spectra in the range of 3700-2700 cm^{-1} , constructed from the FT-IR spectra of set A.

The corresponding asynchronous spectra are shown in Fig. 3b and 4b. All of the peak in Figs. 3b and 4b imply out-of-phase variation between wood bands and coPA bands. In Fig. 4b of set A, one new band is evidenced at 3300 cm^{-1} and the band at 2916 cm^{-1} is splinted in two bands at 2925 and 2891 cm^{-1} .

The bands at 2925 cm^{-1} and 2891 cm^{-1} have out-of-phase variation with wood bands at 3158 cm^{-1} and 3225 cm^{-1} , and most probably come from coPA.

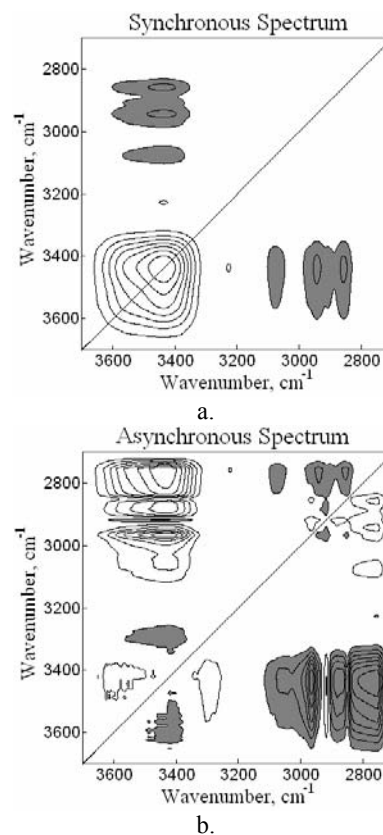


Fig. 4. Synchronous (a) and asynchronous (b) 2D FT-IR correlation spectra in the range of 3700-2700 cm^{-1} , constructed from the FT-IR spectra of set B.

Comparing Figs. 3b and 4b can be observed that the asynchronous bands at 3600, 3225, 3083, 2925, 2891 and 2866 cm^{-1} by set A are shifted to 3566, 3216, 3075, 2916, 2883 and 2850 cm^{-1} in set B. In addition the cross-peaks at 3350 vs 3300 cm^{-1} , 3350 vs 3158 cm^{-1} , 3350 vs 3300 cm^{-1} , 3225 vs 3083 cm^{-1} , 3225 vs 2958 cm^{-1} , 3225 vs 3925 cm^{-1} and 3225 vs 2866 cm^{-1} appear only for set A, while those at 3566 vs 3300 cm^{-1} , 3425 vs 3216 cm^{-1} and 3425 vs 2750 cm^{-1} appear only for set B. All of these peaks should reflect the particular conformational features of set A and set B.

Table 1. Synchronous and Asynchronous 2D correlation intensities and order of intensity variation between two bands of set A.

| No | Φ | Ψ | Assignment | order |
|----|----------------------|----------------------|--------------|------------------|
| 1 | $\Phi(3600, 3083)<0$ | $\Psi(3600, 3083)<0$ | (wood, coPA) | 3600 before 3083 |
| 2 | $\Phi(3600, 2958)<0$ | $\Psi(3600, 2958)<0$ | (wood, coPA) | 3600 before 2958 |
| 3 | $\Phi(3600, 2925)<0$ | $\Psi(3600, 2925)<0$ | (wood, coPA) | 3600 before 2925 |
| 4 | $\Phi(3600, 2891)<0$ | $\Psi(3600, 2891)<0$ | (wood, coPA) | 3600 before 2891 |
| 5 | $\Phi(3600, 2866)<0$ | $\Psi(3600, 2866)<0$ | (wood, coPA) | 3600 before 2866 |
| 6 | $\Phi(1634, 1021)<0$ | $\Psi(1634, 1021)>0$ | (coPA, wood) | 1634 after 1021 |
| 7 | $\Phi(1634, 1089)<0$ | $\Psi(1634, 1089)>0$ | (coPA, wood) | 1634 after 1089 |
| 8 | $\Phi(1544, 1255)<0$ | $\Psi(1544, 1255)>0$ | (coPA, wood) | 1544 after 1255 |
| 9 | $\Phi(1544, 1048)<0$ | $\Psi(1544, 1048)>0$ | (coPA, wood) | 1544 after 1048 |
| 10 | $\Phi(1634, 1255)<0$ | $\Psi(1634, 1255)>0$ | (coPA, wood) | 1634 after 1255 |

Table 2. Synchronous and Asynchronous 2D correlation intensities and order of intensity variation between two bands of set B.

| No | Φ | Ψ | Assignment | order |
|----|----------------------|----------------------|--------------|------------------|
| 1 | $\Phi(3566, 3075)<0$ | $\Psi(3566, 3075)>0$ | (wood, coPA) | 3566 after 3075 |
| 2 | $\Phi(3566, 2883)<0$ | $\Psi(3566, 2883)>0$ | (wood, coPA) | 3566 after 2883 |
| 3 | $\Phi(3566, 2850)<0$ | $\Psi(3566, 2850)>0$ | (wood, coPA) | 3566 after 2850 |
| 4 | $\Phi(3566, 2750)<0$ | $\Psi(3566, 2750)>0$ | (wood, coPA) | 3566 after 2750 |
| 5 | $\Phi(3566, 2916)<0$ | $\Psi(3566, 2916)<0$ | (wood, coPA) | 3566 before 2916 |
| 6 | $\Phi(1641, 1027)<0$ | $\Psi(1641, 1027)<0$ | (coPA, wood) | 1641 before 1027 |
| 7 | $\Phi(1641, 1089)<0$ | $\Psi(1641, 1089)<0$ | (coPA, wood) | 1641 before 1089 |
| 8 | $\Phi(1544, 1255)>0$ | $\Psi(1544, 1255)<0$ | (coPA, wood) | 1544 after 1255 |
| 9 | $\Phi(1544, 1048)<0$ | $\Psi(1544, 1048)<0$ | (coPA, wood) | 1544 before 1048 |
| 10 | $\Phi(1634, 1255)>0$ | $\Psi(1634, 1255)<0$ | (coPA, wood) | 1634 after 1255 |

The order of intensity variation between two bands is listed in Table 1 and table 2 for set A and set B, respectively. In the brackets of each row it is kept the correspondence band and assignment.

The asynchronous peaks at 3600 cm^{-1} vs 3075 cm^{-1} , 3600 cm^{-1} vs 2866 cm^{-1} , and 3600 cm^{-1} vs 2891 cm^{-1} appear in both Fig. 3b and Figure 4b. They have opposite sign from set A to set B (see Table 1-rows 1, 4 and 5 and Table 2- rows 1, 2 and 3). Thus, these asynchronous peaks are symptomatic of the specific interaction in the blends. The band at 3600 cm^{-1} is due to OH stretching vibrations of wood, while the bands at 3075 cm^{-1} and 2866 cm^{-1} are due to NH and CH stretching vibration of coPA. It can conclude that the OH of wood and the NH and CH groups of coPA are involved in the interaction in the blend.

1800 cm^{-1} region. This region is characteristic to C=O, C-O and C-O-C symmetric and asymmetric stretching vibration and also symmetric and asymmetric deformation vibration of aliphatic and aromatic groups.

In synchronous spectrum of set A three autopeaks at 1641 , 1544 and 1040 cm^{-1} , five positive cross-peaks at 1772 vs 1544 cm^{-1} , 1641 vs 1544 cm^{-1} , 1641 vs 1483 cm^{-1} , 1544 vs 1483 cm^{-1} and 1138 vs 1048 cm^{-1} and five negative cross-peaks at 1641 vs 1138 cm^{-1} , 1641 vs 1048 cm^{-1} , 1544 vs 1269 cm^{-1} , 1544 vs 1138 cm^{-1} and 1544 vs 1048 cm^{-1} were evidenced. The band at 1544 cm^{-1} is assigned to amide II of coPA. This band form positive cross-peaks with the band at 1641 cm^{-1} , 1483 cm^{-1} , and 1772 cm^{-1} that means that these bands correspond to the band vibration of coPA.

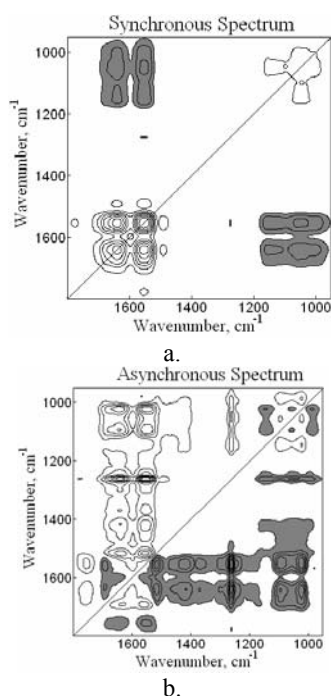


Fig. 5. Synchronous (a) and asynchronous (b) 2D FT-IR correlation spectra in the range of $1800\text{--}900\text{ cm}^{-1}$, constructed from the FT-IR spectra of set A.

Figs. 5a and 6a shows the synchronous and asynchronous correlation spectra for set A and B in 900--

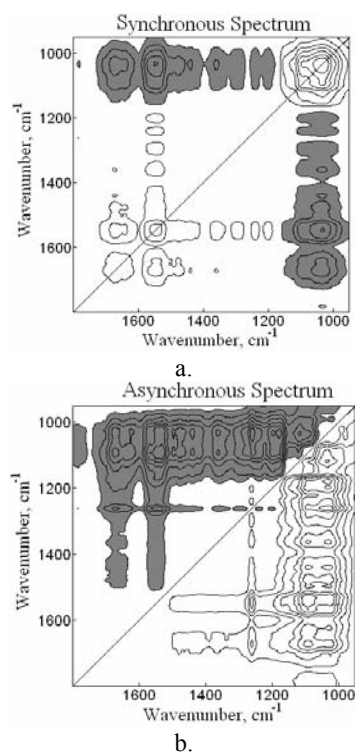


Fig. 6. Synchronous (a) and asynchronous (b) 2D FT-IR correlation spectra in the range of $1800\text{--}900\text{ cm}^{-1}$, constructed from the FT-IR spectra of set B.

The bands at 1269, 1138 and 1048 cm^{-1} form negative cross-peak with the band at 1544 cm^{-1} that means that this bands come from wood.

Synchronous spectrum of set B contains four autopeaks at 1675, 1641, 1544 and 1034 cm^{-1} , twelve positive cross-peaks at 1676 vs 1641 cm^{-1} , 1676 vs 1544 cm^{-1} , 1676 vs 1476 cm^{-1} , 1676 vs 1434 cm^{-1} , 1676 vs 1352 cm^{-1} , 1641 vs 1544 cm^{-1} , 1544 vs 1476 cm^{-1} , 1544 vs 1434 cm^{-1} , 1544 vs 1352 cm^{-1} , 1544 vs 1289 cm^{-1} , 1544 vs 1234 cm^{-1} and 1544 vs 1193 cm^{-1} and ten negative cross-peak at 1779 vs 1034 cm^{-1} , 1676 vs 1034 cm^{-1} , 1641 vs 1034 cm^{-1} , 1544 vs 1034 cm^{-1} , 1476 vs 1034 cm^{-1} , 1434 vs 1034 cm^{-1} , 1352 vs 1034 cm^{-1} , 1289 vs 1034 cm^{-1} , 1234 vs 1034 cm^{-1} and 1193 vs 1034 cm^{-1} . The band at 1544 cm^{-1} assigned to amide II of coPA. form positive cross-peaks with the band at 1476, 1434, 1352, 1641, 1676, 1352, 1289, 1234 and 1193 cm^{-1} , that means that these bands correspond to the band vibration of coPA. The band at 1034 cm^{-1} form negative cross-peak with the band at 1544 cm^{-1} that means that this band come from wood.

The corresponding asynchronous correlation spectra are shown in Figures 5b and Figure 6b.

The asynchronous spectra in this region have a great number of cross-peaks. The asynchronous maps of set A and set B in this region give cross-peaks that have opposite signs, as can be seen by comparing Figure 5b with Figure 6b. The order of intensity variation between some bands of set A and set B are listed in Tables 1 and 2, respectively. The six rows of table 1 and 2 show that the event at 1634 cm^{-1} takes place after and before that at 1021 cm^{-1} in set A and set B, respectively. Thus, the asynchronous peak at 1634 vs. 1021 cm^{-1} in Figure 6b and 7b should arise from the specific interaction that may be responsible for the compatibility of WPC components. The same conclusion is also reached for the asynchronous peaks at 1641 vs. 1089 cm^{-1} and 1544 vs. 1048 cm^{-1} by comparison of the seven and nine rows of Tables 1 and 2. Consequently, the amide bands at 1634 and 1544 cm^{-1} of coPA and the C-O bands at 1021, 1089 and 1048 cm^{-1} of wood are indicative of the specific interaction between wood and coPA.

4. Conclusions

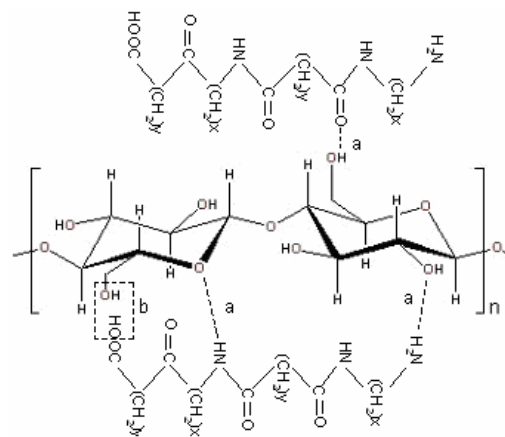
FT-IR spectroscopy and generalized 2D IR correlation spectroscopy has been applied to the study the conformational changes and specific interactions in WPC of wood and coPA.

The 2D synchronous correlation analysis separates the bands of wood from those of coPA and detects bands that are not identifiable from the one-dimensional spectra of wood and coPA.

The 2D asynchronous correlation analysis reveals many out-of-phase band intensity variations that are indicative of the conformational change or the specific interaction in the blends.

1. The bands at 3600 cm^{-1} due to OH stretching vibrations of wood and the bands at 3075 cm^{-1} and 2866 cm^{-1} due to NH and CH stretching vibration of coPA are involved in the interactions in the blends.
2. The amide bands at 1634 and 1544 cm^{-1} of coPA and the C-O bands at 1021, 1089 and 1048 cm^{-1} of wood are

indicative of the specific interaction between wood and coPA, illustrated in scheme 1.



There are at least two kind of possible specific interactions:

- (a) Physical by hydrogen bonding between carbonyl or ester bonds and amide and hydroxyl group of lignocellulosic material (mainly cellulose).
- (b) Chemical interactions appearing at processing temperatures between end groups of coPA and primary -OH groups of cellulose.

Acknowledgement

This work was done under the CEEEX project: "New types of micro- and nanostructured materials for new productions in buildings, bioengineering and food safety" - MAMINAS 3777- financed by MEC.

References

- [1] I. Noda, Appl. Spectrosc. **47**, 1329 (1993).
- [2] I. Noda, Bull. Am. Phys. Soc. **31**, 520 (1986).
- [3] I. Noda, J. Am. Chem. Soc. **111**, 8116 (1989).
- [4] I. Noda, Appl. Spectrosc. **44**, 550 (1990).
- [5] A. Nabet, Pezolet, M. Appl. Spectrosc. **51**, 466 (1997).
- [6] Y. Liu, Y. Ozaki, I. Noda, J. Phys. Chem. **100**, 7327 (1996).
- [7] I. Noda, Y. Liu, Y. Ozaki, J. Phys. Chem. **100**, 8665 (1996).
- [8] Y. Ozaki, Y. Liu, I. Noda, Macromolecules **30**, 2391 (1997).
- [9] M. Muller, R. Buchet, U. P. Fringeli, J. Phys. Chem. **100**, 10810 (1996).
- [10] M. A. Czarniecki, H. Maeda, Y. Ozaki, M. Suzuki, M. Iwahashi, J. Phys. Chem. A **102**, 9117 (1998).
- [11] Y. Wang, K. Murayama, Y. Myojo, R. Tsenkova, N. Hayashi, Y. Ozaki, J. Phys. Chem. B, **102**, 6655 (1998).
- [12] Y. Ren, M. Shimoyama, T. Ninomiya, K. Matsukawa, H. Inoue, I. Noda, Y. Ozaki, (Appl. Spectrosc. **1999**, In press).
- [13] I. Noda, Y. Liu, Y. Ozaki, J. Phys. Chem. **100**, 8674 (1996).

- [14] C. P. Schultz, H. Fabian, H. H. Mantsch, *Biospectroscopy* **4**, 19 (1998).
- [15] Y. Ozaki, Y. Liu, I. Noda, *Appl. Spectrosc.* **51**, 526 (1997).
- [16] T. Nakano, S. Shimada, R. Saitoh, I. Noda, *Appl. Spectrosc* **47**, 1337 (1993).
- [17] H. V. Shah, C. J. Manning, G. A. Arbuckle, *Appl. Spectrosc* **53**, 1542 (1999).
- [18] H. Wang, D. G. Thompson, J. R. Schoonover, S. R. Aubuchon, R. A. Palmer, *Macromolecules* **34**, 7084 (2001).
- [19] V. G. Gregoriou, S. E. Rodman, B. R. Nair, P. T. Hammond, *J. Phys. Chem. B* **106**, 11108 (2002).
- [20] V. G. Gregoriou, S. E. Rodman, B. R. Nair, P. T. Hammond, *Macromol. Symp.* **184**, 183 (2002).
- [21] Y. Nagasaki, T. Yoshihara, Y. Ozaki, *J. Phys. Chem. B* **104**, 2846-2852 (2000).
- [22] S. Morita, Y. Ozaki, I. Noda, *Appl. Spectrosc.* **55**, 1622 (2001).
- [23] L. Sefara, N. P. Magtoto, H. H. Richardson, *Appl. Spectrosc.* **51**, 536 (1997).
- [24] Y. Wang, K. Murayama, Y. Myojo, R. Tsenkova, N. Hayashi, Y. Ozaki, *J. Phys. Chem.* **102** 6655 (1998).
- [25] A. Nabet, M. Pézolet, *Appl. Spectrosc.* **51** 466 (1997).
- [26] B. Hinterstoisser, L. Salmen, *Cellulose* **6**, 251 (1999).
- [27] B. Hinterstoisser, L. Salmen, *Cellulose* **6**, 1 (1999).
- [28] B. Hinterstoisser, M. Akerholm, L. Salmen, *Carbohydr. Res.* **334**, 27 (2001).
- [29] M. Akerholm, L. Salmen, *Polymer* **42**, 963 (2001).
- [30] M. Akerholm, L. Salmen, *J. Pulp Paper Sci.* **28**, 245 (2002).
- [31] C-M. Popescu, Y. Sakata, M-C. Popescu, A. Osaka, C. Vasile, *e-PreservationScience*, 2005; 2: 19 – 29
- [32] http://www.amiplastics.com/ami/Assets/press_releases/newsitem.aspx?item=5.
- [33] A. Crusos, M. Zănoagă: Patent RO, nr. 89603, 1985
- [34] Patent RO, nr. 101323, 1988.
- [35] Y. Mamunya, V. Myshak, E. V. Lebedev, V. Annenkov, *Plast. Massy*, nr. 8, 39-41, (1989).
- [36] Y. P. Mamunya, V. D. Myshak, E. V. Lebedev, (2002), Technologies of polymer-wood composites production using polymer wastes, Proc. 4th Int. Symp. on Wood and Natural Fibre Composites, Kassel, vol. 1, 265-270.
- [37] M. Zănoagă, Y. Mamunya, F. Tanasă, V. Myshak, E. Lebedev, C. Grigoraș, *Materiale Plastice* **42**(4), 272-278 (2005).
- [38] Yanzhi Ren, Tsuyoshi Murakami, Toshikatsu Nishioka, Kenichi Nakashima, Isao Noda, Yukihiko Ozaki, *J. Phys. Chem. B* 2000, 104, 679-690
- [39] N. A. Plate, (Ed.) *Liquid Crystal Polymers*, Plenum Press, New York, 1993.

*Corresponding author cpopescu@icmpp.ro